文章编号：1001－9014(2018)06－0663－05

DOI:10.11972/j.issn.1001－9014.2018.06.004

Hybrid dual wedge plasmonic waveguide with long-range propagation and subwavelength mode confinement

YUE Wen-Cheng, YAO Pei-Jun*, CHEN Xiao-Lin, TAO Run-Xia

(Department of Optics and Optical Engineering, University of Science and Technology of China, Hefei 230026, China)

Abstract: A hybrid dual wedge plasmonic (HDWP) waveguide consisting of two dielectric wedges and a diamond metal wire was proposed. The coupling between dielectric wedge waveguide mode and long-rang surface plasmon polariton mode results in both low propagation loss and ultra-deep-subwavelength confinement. The HDWP waveguide achieves a normalized mode area of 2.9×10^{-3} with a moderate propagation length of 532 μm or a propagation length of 3028 μm with a normalized mode area of 6.2×10^{-3}. The impacts of possible fabrication imperfections on the mode properties are studied. The results indicate that the HDWP waveguide is quite tolerant to fabrication errors.

Key words: waveguide, surface plasmon polariton, photonic integrated circuits

PACS: 42.79.Gn, 78.67.-n, 71.45.Gm

具有长程传播和亚波长模式局域性的混合双楔形等离子体波导

岳文成, 姚培军*, 陈小林, 陶润夏

(中国科学技术大学,光学与光学工程系,安徽 合肥 230026)

摘要:提出一个混合双楔形等离子体波导,该波导由两个楔形介质波导和一个菱形金属线组成.电介质楔形波导模式和长程表面等离子体模式的耦合使得该波导可以获得低损耗的传播和超深的亚波长的模式局域性.混合双楔形等离子体波导在得到一个532 μm的传播长度的同时可以得到一个2.9×10^{-3}的超小的归一化模式面积或者在得到一个6.2×10^{-3}的归一化模式面积的同时可以得到一个3028 μm的超长的传播距离.此外,还研究了制作过程中可能存在的误差对该波导模式性质的影响.计算结果表明,该混合双楔形等离子体波导具有一定的制作容差性.

关 键 词:波导;表面等离子体;光子集成电路

中图分类号:O439 **文献标识码**:A

Introduction

The miniaturization and high-integration density of photonic integrated circuits[1] have always been a significant research subject that attracts many researchers. Surface plasmon polariton (SPP) waveguide is viewed as one of the most promising candidates for large-scale photonic integrated devices, owing to its unique capabilities of breaking the diffraction limit and providing tight light confinement in deep subwavelength scale[2-4]. Many waveguide structures based on SPP have been proposed and studied, such as metal slot SPP waveguides[5-8], V-groove channel SPP waveguides[9-11], and wedge SPP waveguides[12-16]. These SPP waveguides could offer tight confinement of light but suffer enormous propagation loss due to the metallic ohmic loss[17]. In order to improve the trade-off between mode confinement and propagation loss, several hybrid plasmonic waveguides have been proposed[18-26]. These hybrid plasmonic waveguides guide light not only by the SPP along the metal/dielectric interface but also by the dielectric index contrast near the

Received date: 2018-03-09, **revised date**: 2018-09-27 **收稿日期**:2018-03-09, **修回日期**:2018-09-27

Foundation items: Supported by National Key Basic Research Program of China (2012CB922003), National Natural Science Foundation of China (61177053), and Anhui Provincial Natural Science Foundation (1508085SMA205)

Biography: YUE Wen-Cheng(1989-), female, Dezhou, China, Ph. D. Research area focuses on the design and simulation of micro-/nano-optics devices. E-mail: wchengy@mail.ustc.edu.cn

* **Corresponding author**: E-mail: yap@ustc.edu.cn

metal surface as well. The hybridization between dielectric waveguide mode and pure SPP mode could be tuned by changing waveguide parameters. Then the characteristics of the hybrid mode could be transformed from SPP-like to dielectric-like. In this paper, we design a hybrid dual wedge plasmonic (HDWP) waveguide which is composed of two identical dielectric wedge waveguides and a diamond metal wire, these two wedge waveguides are symmetrically placed on two opposed wedges of the diamond metal wire. Compared with the previous long-range hybrid wedge plasmonic (LRHWP) waveguide[26], our HDWP waveguide can provide stronger mode confinement for similar propagation length or longer propagation length for alike mode confinement. Possible practical fabrication imperfections of the proposed HDWP waveguide are also investigated in detail.

1 Waveguide structure and mode properties

Figure 1 illustrates the geometry of our proposed HDWP waveguide, where two identical silicon (Si) wedge waveguides (SWWs) with a height of H are symmetrically placed on two opposed wedges of a diamond silver (Ag) wire with a small gap g, and the surrounding low-index dielectric material is silica (SiO_2). The tip of the Si wedge has an angle of α and a curvature radius of r. The diamond Ag wire has a fixed cross section area of 1 200 nm^2[26], and its tip has an angle of θ and a curvature radius of r. The typical value of the curvature radius is selected as $r = 10$ nm[27] by considering practical fabrication conditions. The working wavelength is 1 550 nm in our simulations. The corresponding permittivities of SiO_2, Si and Ag are $\epsilon_c = 2.25$, $\epsilon_d = 12.25$ and $\epsilon_m = -129 + 3.3i$, respectively[25, 28]. The mode properties of the proposed HDWP waveguide are studied using the finite-element method (FEM) with the perfectly matched layer (PML) boundary condition.

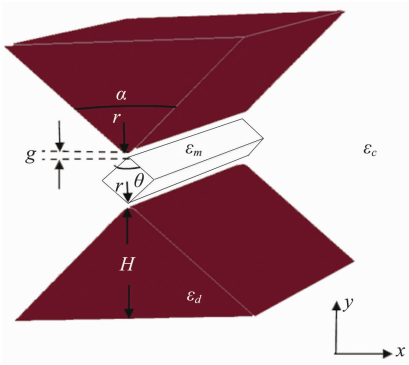

Fig. 1 Schematic illustration of the proposed HDWP waveguide
图1 HDWP波导的结构示意图

Figures 2(a-b) show the propagation length (L_p) and normalized mode area (A_{eff}/A_0) of the HDWP waveguide as functions of the Si wedge height H at different gap g. In this simulation, the parameters used are $\theta = \alpha = 100°$. The propagation length and normalized mode area both decrease at first and then increase along with H. When H changes from 150 nm to 200 nm, the propagation length and normalized mode area both achieve smaller values. For $H > 200$ nm, the HDWP waveguide supports a low-loss SWW-like mode with electromagnetic energy restricted to the high-permittivity Si wedge core [Figs. 2(c-d)][18]. Inversely, the HDWP waveguide mode behaves as a LRSPP-like mode for $H <$ 150 nm [Figs. 2(g-h)], resulting in a long propagation length and a large mode area[18]. At moderate Si wedge height (H changing from 150 nm to 200 nm), mode coupling leads to a new hybrid mode that features both SWW mode and LRSPP mode characteristics [Figs. 2(e-f)][18]. In addition, the propagation length and normalized mode area both increase along with the gap g [Figs. 2(a-b)]. It is worth mentioning that most of the hybrid mode energy becomes strongly confined in the SiO_2 gap region as the gap g decreases to the nanometer scale [Figs. 2(d), (f), and (h)]. Compared with the LRHWP waveguide (parameters of the LRHWP waveguide are $\theta = 140°$, $h = 2$ nm, and $d = 240$ nm)[26], our HDWP waveguide can achieve similar propagation length of 532 μm at $H = 200$ nm $g = 2$ nm, while the normalized mode area of 2.9×10^{-3} of the HDWP waveguide is about 2.3 times smaller than the LRHWP waveguide[26].

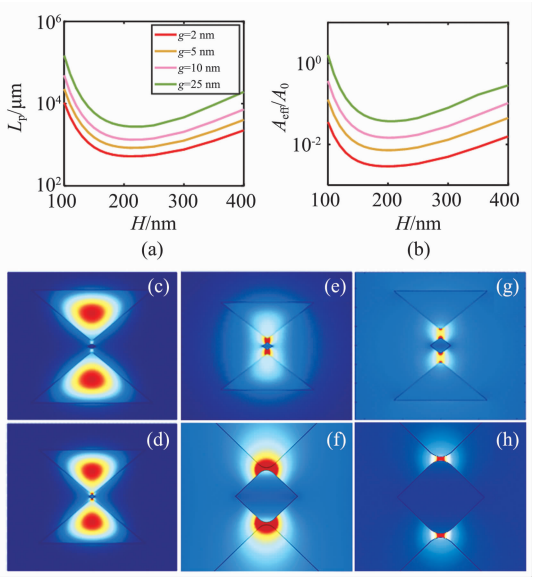

Fig. 2 (a) Propagation length (L_p) and (b) normalized mode area (A_{eff}/A_0) as functions of the Si wedge height H with different gap g. (c)-(h) Electromagnetic energy density distributions: (c) [H, g] = [400, 25] nm, (d) [H, g] = [400, 2] nm, (e) [H, g] = [200, 25] nm, (f) [H, g] = [200, 2] nm, (g) [H, g] = [100, 25] nm, and (h) [H, g] = [100, 2] nm
图2 (a)传播长度和(b)归一化模式面积在不同的g处随着H的变化情况,(c)-(h)电磁场能量密度的分布情况,对应[H, g]的取值依次为:(c)[400, 25] nm, (d)[400, 2] nm, (e)[200, 25] nm, (f)[200, 2] nm, (g)[100, 25] nm, (h)[100, 2] nm

To get a deeper understanding, we show the dependence of the hybrid mode's effective refractive index

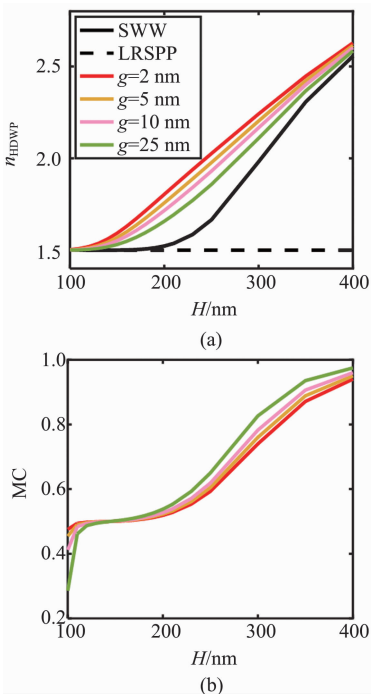

Fig. 3　Dependence of (a) the hybrid mode's effective refractive index (n_{HDWP}) of the HDWP waveguide and (b) the mode character (MC) determined by Eq. 1 on the Si wedge height H and gap g. The black solid line and black dash line in (a) represent the effective refractive indices of the SWW and LRSPP modes, respectively

图 3　(a)混合模式的有效折射率和(b)模式特性随着 H 和 g 的变化情况,(a)中的黑色实线和虚线分别代表 SWW 和 LRSPP 模式的有效折射率

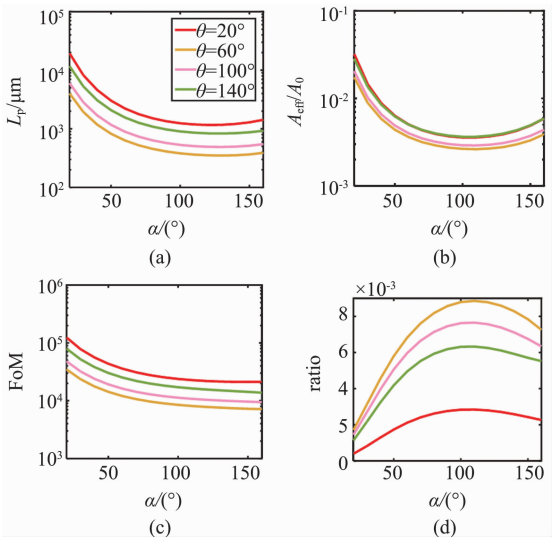

Fig. 4　Dependence of (a) propagation length (L_P), (b) normalized mode area (A_{eff}/A_0), (c) figure of merit (FoM), and (d) the ratio of the electromagnetic energy in the metal region to the total electromagnetic energy of the HDWP waveguide on the Si wedge tip angle α at different θ

图 4　(a)传播长度、(b)归一化模式面积、(c) FoM、和(d)金属中的电磁能量占总能量的比例在不同的 θ 处随着角度 α 的变化情况

of the HDWP waveguide (n_{HDWP}) on H and g in Fig. 3 (a). The chosen parameters in Fig. 3 is the same as Fig. 2. The hybrid mode's effective index approaches to the refractive index of the SWW or LRSPP mode in the limit of SWW-like or LRSPP-like mode, respectively. The mode hybridization can be studied using the coupled-mode theory in Ref. [18], where the mode character (MC) is defined as

$$\mathrm{MC} = \frac{n_{HDWP} - n_{LRSPP}}{(n_{HDWP} - n_{LRSPP}) + (n_{HDWP} - n_{SWW})} \quad (1)$$

where n_{LRSPP} and n_{SWW} are respectively the effective refractive indices of the LRSPP mode and SWW mode. In this regard, the mode is SWW-like for MC > 0.5 and LRSPP-like otherwise. As shown in Fig. 3(b), MC is about 0.5 when H varies from 150 nm to 200 nm, indicating the strongest coupling between the SWW and LRSPP modes. When H > 200 nm (H < 150 nm), MC > 0.5 (MC < 0.5), the mode is SWW-like (LRSPP-like), which is consistent with the above analysis.

The dependence of propagation length (L_P), normalized mode area (A_{eff}/A_0), and figure of merit (FoM)[29-30] on α at different θ is shown in Figs. 4 (a-c), respectively. The Si wedge height H and gap g are respectively set as 200 nm and 2 nm in this simulation. The propagation length and normalized mode area both decrease firstly and then increase with an increase in α or θ. The normalized mode area at $\theta = \alpha = 100°$ is little larger than the minimum value at $\theta = 60°$ $\alpha = 100°$, but the FoM at $\theta = \alpha = 100°$ is larger than that at $\theta = 60°$ $\alpha = 100°$ (Fig. 4(c)), that is why we set $\theta = \alpha = 100°$ in Fig. 2. To understand the behavior of the propagation length, we depict the ratio of the electromagnetic energy in the diamond metal region to the total electromagnetic energy of the HDWP waveguide in Fig. 4 (d). The ratio increases and then decrease as α or θ increases, which is opposite to the change of propagation length. This is consistent with our knowledge that the smaller the ratio, the less the loss and the longer the propagation length. Compared with the LRHWP waveguide (parameters of the LRHWP waveguide are $\theta = 140°$, $h = 2$ nm, and $d = 240$ nm)[26], our HDWP waveguide can obtain similar normalized mode area of 6.2×10^{-3} at $\theta = 20°$ $\alpha = 50°$, while the propagation length of 3028 μm of the HDWP waveguide is about 4.6 times longer than the LRHWP waveguide[26].

2　Analysis of fabrication error tolerance

It is difficult to fabricate perfect HDWP waveguide structure considering practical fabrication conditions. Hence, it is necessary to analyze possible practical fabrication imperfections (i.e., fabrication error tolerance) including misalignment between the diamond metal wire and the Si wedge, asymmetric positioning of two Si wedges with respect to the metal wire, and tilt or rotation of the metal wire. In all analyses of fabrication error tolerance, the HDWP waveguide parameters used are $g = 2$ nm, $H = 200$ nm, and $\theta = \alpha = 100°$.

2.1　Misalignment along the horizontal direction

The deviation of Si wedges from the diamond metal

wire might affect the mode properties. There are three kinds of misalignment along the horizontal direction, as illustrated in Figs. 5 (a-c). Figures 5(d) and (e) respectively show the influence of the three types of misalignment on propagation length and normalized mode area, where the insets are the corresponding normalized electromagnetic energy density distributions. The proposed HDWP waveguide suffers less than 20% variation of propagation length and about 10% undulation of normalized mode area under 10 nm misalignment for misalignment 1. For misalignment 2 and 3, the propagation length is subjected to < 8% fluctuation and the mode area sustains < 20% undulation under 4 nm misalignment.

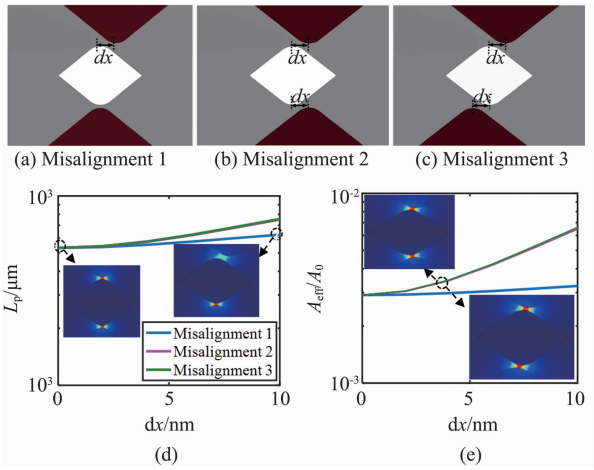

Fig. 5 Schematic views of (a-c) three kinds of misalignment along the horizontal direction and influence of the three types of misalignment on (d) propagation length (L_P) and (e) normalized mode area (A_{eff}/A_0). Insets: the normalized electromagnetic energy density distributions

图5 (a-c)水平方向三种不对齐方式的示意图以及这三种不对齐方式对(d)传播长度和(e)归一化模式面积的影响,其中的插图给出了归一化电磁场能量密度的分布

2.2 Asymmetry in the vertical direction

The asymmetry of two Si wedges with respect to the metal wire, i. e., different distance of upper and lower gap, might have effect on the mode properties. Figures 6 (a-b) show the dependence of propagation length and normalized mode area on one gap changing from 2 nm to 12 nm and the other gap setting at 2 nm. As one of the gaps increases from 2 nm to 12 nm, the propagation length changes from 532 μm to 726 μm and the normalized mode area varies from 2.9×10^{-3} to 4.6×10^{-3}. Insets in Figs. 6(a-b) are the corresponding normalized electromagnetic energy density distributions.

2.3 Tilt or rotation of the metal wire

The diamond metal wire may rotate from its center point with an angle dθ, which might influence the mode properties. Figures 7(a-b) show that the proposed HDWP waveguide suffers about 3% fluctuation of propagation length and approximately 10% variation of normalized mode area under 10° tilt or rotation of the metal wire.

The obtained results suggest that the practical fabrication imperfections in geometry parameters like slight misalignment along the horizontal direction, asymmetry in the vertical direction, and tilt or rotation of the metal wire have modest influences on the mode properties.

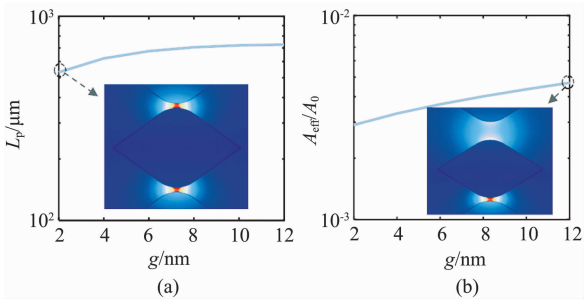

Fig. 6 Influence of the asymmetry in the vertical direction (different distance of upper and lower gap) on (a) propagation length (L_P) and (b) normalized mode area (A_{eff}/A_0). Insets: the normalized electromagnetic energy density distributions

图6 垂直方向的不对称对(a)传播长度和(b)归一化模式面积的影响,其中的插图给出了归一化电磁场能量密度的分布

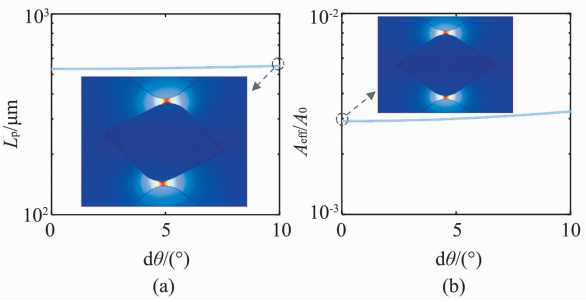

Fig. 7 Influence of tilt or rotation of the metal wire on (a) propagation length (L_P) and (b) normalized mode area (A_{eff}/A_0). Insets: the normalized electromagnetic energy density distributions

图7 金属线的倾斜或旋转对(a)传播长度和(b)归一化模式面积的影响,其中的插图给出了归一化电磁场能量密度的分布

3 Conclusions

We demonstrate a HDWP waveguide composed of two identical triangular wedges which are symmetrically placed on a diamond metal wire, and investigate the influence of the geometrical parameters on the propagation length and normalized mode area. Compared with the LRHWP waveguide mentioned above, our proposed HDWP waveguide has better performance. In other words, with similar propagation length, the normalized mode area for the HDWP waveguide is approximately 2.3 times smaller than that of the LRHWP waveguide; and with analogous mode confinement, the propagation length of our HDWP waveguide is about 4.6 times longer than that of the aforementioned LRHWP waveguide. Moreover, our designed HDWP waveguide has good tolerance to the possible fabrication imperfections, including misalignment along the horizontal direction, asymmetry in the vertical direction, and tilt of the metal wire. The favorable performance of our HDWP waveguide makes them va-

rious potential applications in subwavelength devices, such as nanophotonic waveguides, optical tweezers, nanolasers, and so on.

Methods

The propagation length (L_P), defined as the distance for the SPP intensity to decay by a factor of $1/e$[31], is calculated by

$$L_P = \lambda/[4\pi\,\mathrm{Im}(n_{\mathrm{eff}})] \quad , \quad (2)$$

where $\mathrm{Im}(n_{\mathrm{eff}})$ is the imaginary part of the effective refractive index and n_{eff} is calculated by FEM.

The normalized mode area is defined by A_{eff}/A_0, where A_0 is the diffraction-limited mode area and defined as $\lambda^2/4$, and the effective mode area A_{eff} is evaluated by[18]

$$A_{\mathrm{eff}} = \frac{1}{\max\{W(\boldsymbol{r})\}}\iint W(\boldsymbol{r})\,\mathrm{d}^2\boldsymbol{r} \quad , \quad (3)$$

where $W(\boldsymbol{r})$ is the electromagnetic energy density and is given by

$$W(\boldsymbol{r}) = \frac{1}{2}\left\{\frac{\mathrm{d}[\epsilon(\boldsymbol{r})\omega]}{\mathrm{d}\omega}|\boldsymbol{E}(\boldsymbol{r})|^2 + \mu_0|\boldsymbol{H}(\boldsymbol{r})|^2\right\} . \quad (4)$$

The figure of merit (FoM) is the ratio of the propagation length to the diameter of effective mode area[32]

$$\mathrm{FoM} = L_P/(2\sqrt{A_{\mathrm{eff}}/\pi}) \quad . \quad (5)$$

FoM is an important parameter that provide a proper assessment for the trade-off between the propagation length and effective mode area.

Acknowledgments

This work was supported by National Key Basic Research Program of China (grant no. 2012CB922003); National Natural Science Foundation of China (grant no. 61177053); and Anhui Provincial Natural Science Foundation (grant no. 1508085SMA205).

References

[1] Ebbesen T W, Genet C, Bozhevolnyi S I. Surface-plasmon circuitry [J]. *Physics Today*, 2008, **61**(5):44-50.
[2] Wang J. A review of recent progress in plasmon-assisted nanophotonic devices [J]. *Frontiers of Optoelectronics*, 2014, **7**(3): 320-337.
[3] Barnes W L, Dereux A, Ebbesen T W. Surface plasmon subwavelength optics [J]. *Nature*, 2003, **424**(6950): 824-830.
[4] Gramotnev D K, Bozhevolnyi S I. Plasmonics beyond the diffraction limit [J]. *Nature Photonics*, 2010, **4**(2): 83-91.
[5] Veronis G, Fan S. Guided subwavelength plasmonic mode supported by a slot in a thin metal film [J]. *Optics Letters*, 2005, **30**(24): 3359-3361.
[6] Pile D F, Ogawa T, Gramotnev D K, *et al*. Two-dimensionally localized modes of a nanoscale gap plasmon waveguide [J]. *Applied Physics Letters*, 2005, **87**(26):261114-26114.
[7] Liu L, Han Z, He S. Novel surface plasmon waveguide for high integration [J]. *Optics Express*, 2005, **13**(17):6645-6650.
[8] Dionne J, Sweatlock L, Atwater H, *et al*. Plasmon slot waveguides: Towards chip-scale propagation with subwavelength-scale localization [J]. *Physical Review B*, 2006, **73**(3):035407-035407.
[9] Zenin V A, Volkov V S, Han Z, *et al*. Dispersion of strongly confined channel plasmon polariton modes [J]. *Journal of the Optical Society of America B*, 2011, **28**(7):1596-1602.
[10] Bozhevolnyi S I, Volkov V S, Devaux E, *et al*. Channel plasmon subwavelength waveguide components including interferometers and ring resonators [J]. *Nature*, 2006, **440**(7083):508-511.
[11] Moreno E, García-Vidal F J, Rodrigo S G, *et al*. Channel plasmon-polaritons: modal shape, dispersion, and losses [J]. *Optics Letters*, 2006, **31**(23):3447-3449.
[12] Pile D F P, Ogawa T, Gramotnev D K, *et al*. Theoretical and experimental investigation of strongly localized plasmons on triangular metal wedges for subwavelength waveguiding [J]. *Applied Physics Letters*, 2005, **87**(6):061106-061106.
[13] Moreno E, Rodrigo S G, Bozhevolnyi S I, *et al*. Guiding and focusing of electromagnetic fields with wedge plasmon polaritons [J]. *Physical Review Letters*, 2008, **100**(2):023901-023901.
[14] Boltasseva A, Volkov V S, Nielsen R B, *et al*. Triangular metal wedges for subwavelength plasmon-polariton guiding at telecom wavelengths [J]. *Optics Express*, 2008, **16**(8):5252-5260.
[15] Ogawa T, Pile D F P, Okamoto T, *et al*. Numerical and experimental investigation of wedge tip radius effect on wedge plasmons [J]. *Journal of Applied Physics*, 2008, **104**(3):033102-033102.
[16] Mu J, Chen L, Li X, *et al*. Hybrid nano ridge plasmonic polaritons waveguides [J]. *Applied Physics Letters*, 2013, **103**(13):131107-131107.
[17] Zia R, Selker M D, Catrysse P B, *et al*. Geometries and materials for subwavelength surface plasmon modes [J]. *Journal of the Optical Society of America A*, 2004, **21**(12):2442-2446.
[18] Oulton R F, Sorger V J, Genov D A, *et al*. A hybrid plasmonic waveguide for subwavelength confinement and longrange propagation [J]. *Nature Photonics*, 2008, **2**(8):496-500.
[19] Dai D, He S. A silicon-based hybrid plasmonic waveguide with a metal cap for a nano-scale light confinement [J]. *Optics Express*, 2009, **17**(19):16646-16653.
[20] Bian Y, Zheng Z, Zhao X, *et al*. Symmetric hybrid surface plasmon polariton waveguides for 3D photonic integration [J]. *Optics Express*, 2009, **17**(23):21320-21325.
[21] Avrutsky I, Soref R, Buchwald W. Sub-wavelength plasmonic modes in a conductor-gap-dielectric system with a nanoscale gap [J]. *Optics Express*, 2010, **18**(1):348-363.
[22] Bian Y, Zheng Z, Liu Y, *et al*. Dielectric-loaded surface plasmon polariton waveguide with a holey ridge for propagation-loss reduction and subwavelength mode confinement [J]. *Optics Express*, 2010, **18**(23):23756-23762.
[23] Chen L, Zhang T, Li X, *et al*. Novel hybrid plasmonic waveguide consisting of two identical dielectric nanowires symmetrically placed on each side of a thin metal film [J]. *Optics Express*, 2012, **20**(18): 20535-20544.
[24] Xiang C, Wang J. Long-range hybrid plasmonic slot waveguide [J]. *IEEE Photonics Journal*, 2013, **5**(2): 4800311-4800311.
[25] Bian Y, Zheng Z, Liu Y, *et al*. Hybrid wedge plasmon polariton waveguide with good fabricationerror-tolerance for ultra-deep-subwavelength mode confinement [J]. *Optics Express*, 2011, **19**(23):22417-22422.
[26] Zhang Z, Wang J. Long-range hybrid wedge plasmonic waveguide [J]. *Scientific Reports*, 2014, **4**(1):6870-6870.
[27] Yan M, Qiu M. Guided plasmon polariton at 2D metal corners [J]. *Jornal of the Optical Society America B*, 2007, **24**(9):2333-2342.
[28] Johnson P B, Christy R W. Optical constants of the noble metals [J]. *Physical Review B*, 1972, **6**(12):4370-4379.
[29] Buckley R, Berini P. Figures of merit for 2D surface plasmon waveguides and application to metal stripes [J]. *Optics Express*, 2007, **15**(19):12174-12182.
[30] P. Berini. Figures of merit for surface plasmon waveguides [J]. Optics Express, 2006, **14**(26):13030-13042.
[31] Oulton R F, Bartal G, Pile D F P, *et al*. Confinement and propagation characteristics of subwavelength plasmonic modes [J]. *New Journal of Physics*, 2008, **10**(10):105018-105018.
[32] Berini P. Long-range surface plasmon polaritons [J]. *Advances in Optics and Photonics*, 2009, **1**(3):484-588.